COMPDYN 2015
5th ECCOMAS Thematic Conference on
Computational Methods in Structural Dynamics and Earthquake Engineering
M. Papadrakakis, V. Papadopoulos, V. Plevris (eds.)
Crete Island, Greece, 25–27 May 2015

A CODE COMPATIBLE APPROACH TO JUSTIFY THE SEISMIC DESIGN OF SIMPLIFIED STRUCTURES

H.F. Karadogan[1], Y. Durgun[2], I.E. Bal[3], S. Z. Yuce[4], E. Yuksel[5], C. Soydan[6]

[1] Emer. Prof.
Faculty of Civil Engineering, Istanbul Technical University (ITU), Istanbul, Turkey,
karadogan@itu.edu.tr

[2] Dr., [5]Assoc. Prof
Faculty of Civil Engineering, ITU, Istanbul, Turkey
durgunya@itu.edu.tr, yukselerc@itu.edu.tr

[3]Asst. Prof
Earthquake Eng. & Disaster Management Institute, ITU, Istanbul, Turkey
iebal@itu.edu.tr

[4]Dr. , [6] Ph.D. Candidate
Graduate School of Science Engineering and Technology of ITU, Istanbul, Turkey
yuceser@itu.edu.tr, cihansoydan@gmail.com

Keywords: Column Design, Precast Structures, Single Story Frames, Buckling, NTHA

Abstract

An attempt to find out the most probable displacement demands of precast cantilever columns has been presented here. The purpose of the findings presented is to set up a more reliable design philosophy based on dynamic displacement considerations instead of using acceleration spectrum based design which initiates the action with unclear important assumptions such as the initial stiffness, displacement ductility ratio etc. The sole aim of this paper is to define a procedure for overcoming the difficulties rising right at the beginning of the traditional design procedure. For that purpose first 12 groups of earthquake records cover the cases of far field, near field, firm soil, soft soil possibilities for 2/50, 10/50 and 50/50 earthquakes with minimum scale factors are identified associated to the present fundamental period of structure. And they are reselected for each new period of structure during the iterative algorithm presented here and they are used to remove the displacement calculations based on static consideration.

Nonlinear Time History Analysis (NLTHA) are employed within the algorithm presented here which takes into account the strength and stiffness degradations of structural elements and the duration of records which are ignored in the spectrum based design philosophy.

1 INTRODUCTION

Single story precast frame type structures are widely used in the construction of industrial facilities and commercial malls in Turkey. The non-moment resisting *beam-to-column connections* are all wet connections. The lateral strength and stiffness of the structure depend entirely on the cantilevered columns, see. Fig. 1.

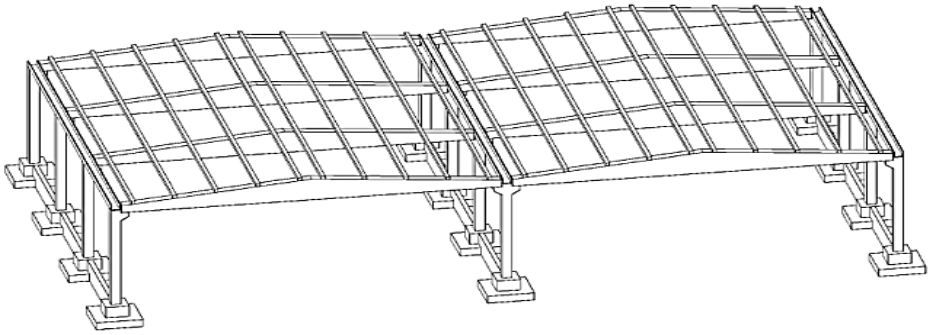

Fig. 1 Single story precast frame type structure

After August 1999 Kocaeli and November 1999 Düzce Earthquakes, site investigations revealed that structural *damage* and *collapse* of one-story precast structures were common especially in uncompleted structures, [1,2,3,4,5]. Various types of structural damage were frequently observed in one-story precast structures, such as plasticized zones at the base of the columns, axial movement of the roof girders that led to pounding against the supporting columns or falling of the roof girders, [6]. The post-earthquake observations of one-story precast frame type structures indicate also that

- Lateral stiffness may not be high enough to limit the lateral displacement of column tops which may differ from peripheral columns to center columns simply because of the lack of in-plane rigidity of roofing system, Fig. 2a,
- Hence the excessive top rotations of columns and the relative displacement in the plane of roof become perfect reasons to dislocate the long span heavy slender roof beam together with the other two component of earthquake, Fig. 2b. They are creating perfect imperfections as well, for out of plane buckling of beams which have very simple insufficient hinge connections to the columns.
- Incompatible column displacement ductility achieved in the field and the lateral load reduction factor used in design, Fig. 2c.

(a) (b) (c)

Fig. 2 Observed damages

In addition to the observations listed above it is also known that, structural alterations done after construction, the effects of nonstructural elements used unconsciously, oversimplified details of connections can be counted among the other important deficiencies of these buildings which causes severe damages.

At the design stage of that type of buildings, the seismic weight coming from the tributary area of columns are determined easily for predicting the earthquake loads. However the *Lateral Displacement Ductility Ratio* which is the main parameter of *Lateral Load Reduction Factor* has to be selected at the beginning of design which is not an easy estimation and has its own uncertainties. Another difficulty is to estimate the lateral rigidity of column which is going to be used to calculate the fundamental period of vibration to go to the spectrum curves. Finally the proposed displacement limits based on static considerations are no longer satisfying the requirements of dynamic displacement calculations.

Those are the factors which are being discussed following experimental and theoretical primary works, [7,8,9]. This Chapter is the scrutinized summary of the findings of the earlier works of the Authors and is aimed to establish a conclusive design algorithm as proposed below.

2 BASIC STRUCTURAL FEATURES OBSERVED IN THE FIELD AND BASIC FEATURES OF THE CURRENT DESIGN PRACTICE

It is strongly probable that all the above mentioned damaged and collapsed buildings they have been neither designed nor manufactured nor mounted properly. From structural engineering point of view, the following facts are important to critic the present design practice:

- Generally there exist almost no in–plane rigidity in the roof and in the sides of the examined precast buildings.
- Generally the connections between the long span beams and columns are almost hinged and they are vulnerable to different types of failure modes in addition to shear strength deficiency such as rupture of concrete around the shear studs etc.
- Generally the tributary areas of columns are used to define the earthquake design forces. When this come along the lack of in-plane rigidity of roof then columns in different location with different dynamic characteristics starts to behave independently hence top displacements and top rotations in opposite direction becomes an important issue to keep the long span and heavy roof beam in the required position. Because all kind of imperfection to destabilize the roof beam appears in addition to the inherent tendency towards out of plane buckling.

In local design practice generally un-cracked sections are used to calculate the fundamental period of the structure. Static calculations are required for determination of displacements and a lateral load reduction factors suggested by codes are used to define the design loads.

One of the main issues in precast structures is that the top displacement of center columns in precast single story industrial buildings may not have synchronized seismic oscillations with the perimeter columns despite the fact that they often have the same cross sectional dimensions. The precast industrial structures do not possess in-plane rigidity at roof level in most cases leading thus to lack of load path among the columns resulting individual shaking of each column [10]. The displacement time-history plots of Column #1, the details of which are given below in the section of *Numerical Analyses*, are presented in Fig. 3. The bottom plot in Fig. 3 presents that the maximum center column displacement is 26 cm, while the middle column maximum displacement is 20 cm. These two numbers may mislead the engineer to a

wrong conclusion that the differential displacement between the perimeter and center columns is just 26-20=6 cm. If the top plot with the differential displacement between the two columns in time domain is observed, however, it can be seen that the maximum differential (i.e. asyncronized) displacement reaches up to level of 33 cm. The main reason for that is because the top displacement of each individual column may occur at different time steps thus the phase alteration may cause large asyncronized displacements. In other words, the top displacement of a center and of a perimeter column may have opposite signs.

The top displacement of individual cantilever columns exhibiting opposite signs may lead to instability of the beams which are hinged to the column tops in existing practice. It can be seen in Fig. 4 following analyses of perimeter and center columns of a single-story precast structure with 20 code-compatible records that the tip rotation is always higher than the chord rotation (please note that the chord rotation is equal to drift in cantilever systems). In other words, the tip of the column where hinged beams are connected rotates more than the column itself. This is a major parameter neglected in design.

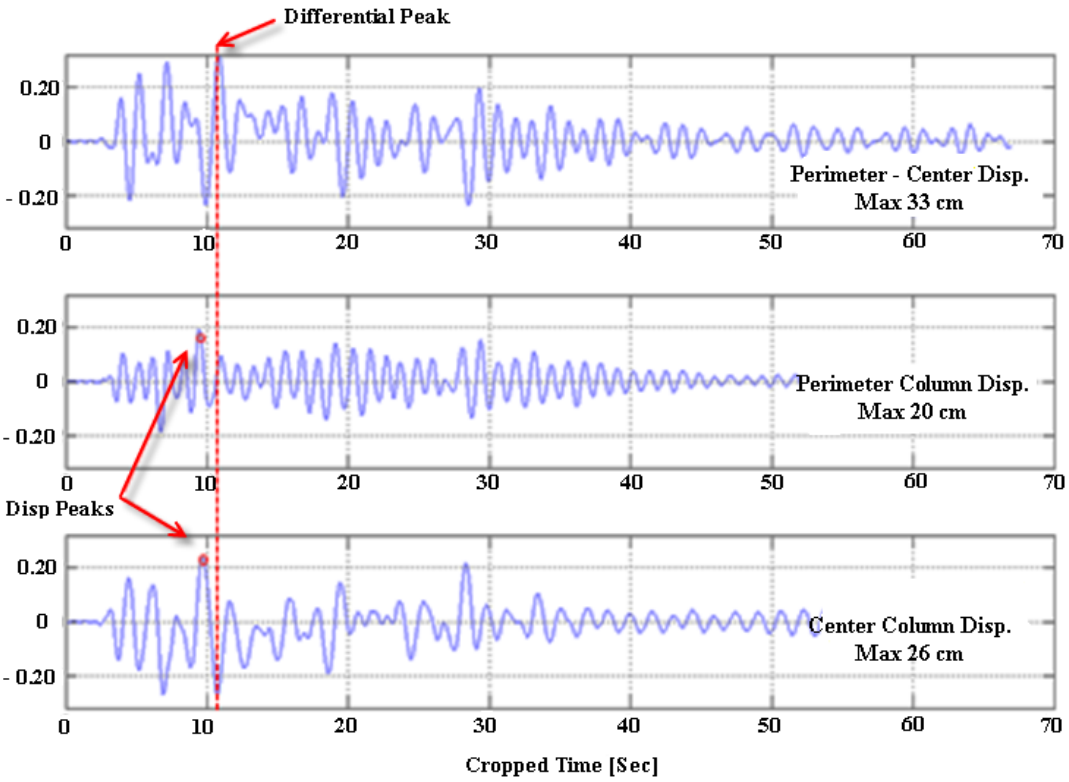

Fig. 3 Asynchronized displacement time histories for center and perimeter columns of a single-story precast Structure

3 WHY JUSTIFICATION OF CODE BASED DESIGN PROCEDURE IS NEEDED?

Even if the damaged or collapsed buildings shown in Fig. 2 had been designed properly, been manufacured properly and been mounted properly, unless the assumptions done at the beginning of design are not justified at the end, one should have rigth to keep suspition about the safety of building.

The basic questions to be kept in mind till the satisfactory design has been reached, are as follows:

- What should be the initial period of the structure on which the fundamental period will be based?
- What should be the displacement ductility factor or lateral load reduction factor on which the design forces will be based?
- To what extent is valid the story drift calculation based on static considerations?

One of the other deficiencies of spectrum based design technique is the length of the record which is not taken into account and the other one is the stiffness and strength deterioration of structure: Unfortunately they are not embedded in the procedure widely used by existing codes.

In order to satisfy the suspicions from which all those questions are arising, an algorithm to justify the design procedures used at the beginning, is presented in the following paragraphs.

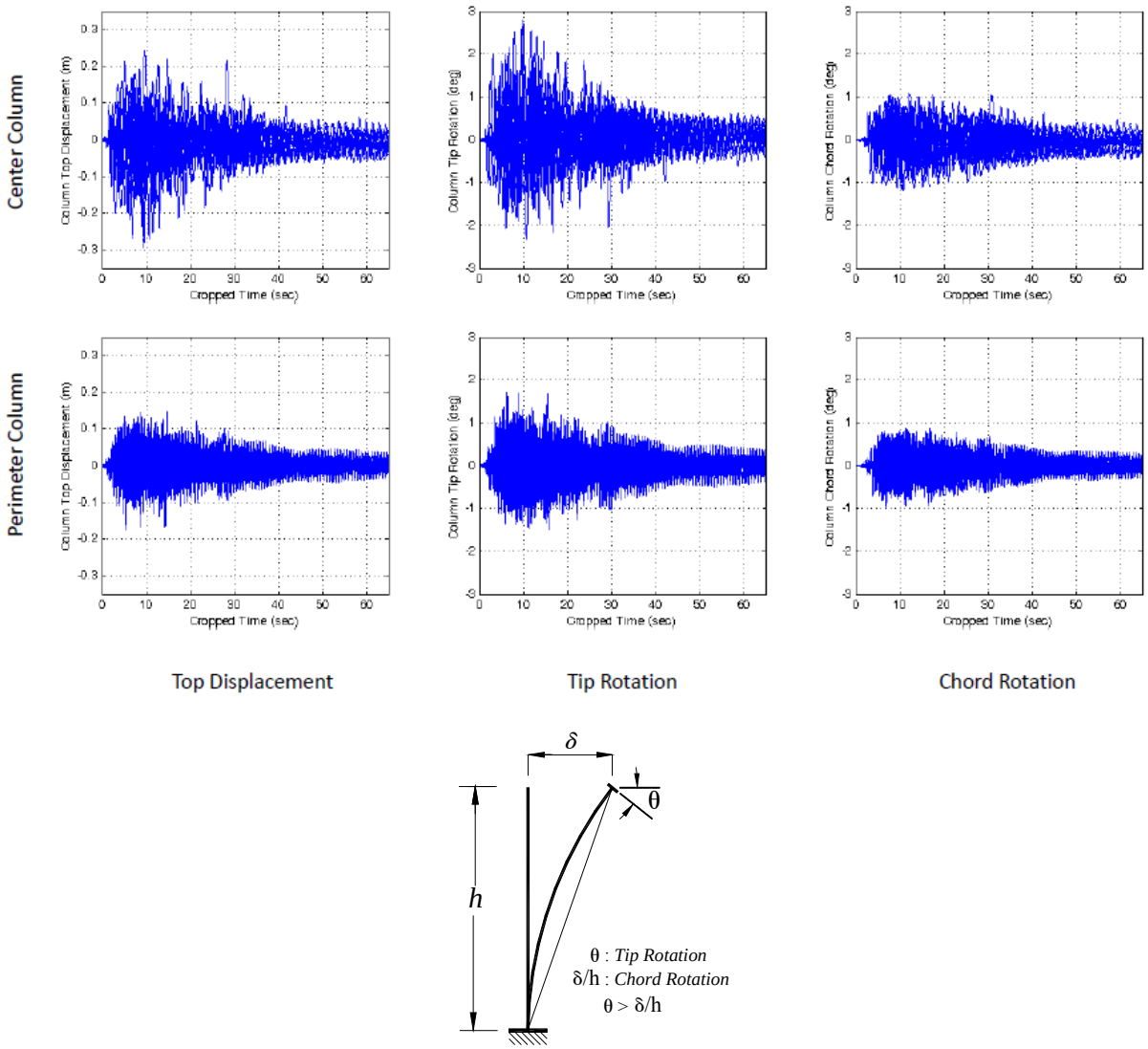

Fig. 4 Definition of *chord rotation* and *tip rotations* (top), comparison of top displacement, tip rotation and chord rotation quantities for an example precast industrial structure (bottom)

4 SELECTION OF PARTIALLY CODE COMPATIBLE RECORDS

A simple engineering approach is used here for the selection of records used in nonlinear analyses. The record selection has been done by using the PEER NGA database [11] where 7025 recorded motions were available. An in-house developed software was used to list and download the record automatically and plot the spectra for acceleration at 5% damping, velocity and displacement.

Twelve bins of records, [12], are created where:

1. Earthquake intensity (2/50, 10/50 or 50/50 earthquakes, 3 bins)
2. Far field or near field issue (2 bins)
3. Soil type (firm soil and soft soil, 2 bins)

parameters are checked. Each of these 12 bins have 20 records,

In terms of the selection algorithm, first the acceleration spectrum of the original record is compared to that of the target, in the period window of 0.2 to 2.0 sec. A scale factor is applied to the ordinates. Then the near field vs. far field comparison is made where the distances above 15 km are assumed as far field. Finally a comparison is made in terms of the soil type where the records taken on soil with Vs30 higher than 300 m/sec are assumed to be recorded on firm soil while records taken on soils with Vs30 lower than 700 m/sec are assumed to be recorded on soft soil. There is certainly an overlap in the soil criteria; this is nevertheless unavoidable if one checks the firm and soft soil borders in the guidelines and codes.

The intensity levels of 2/50, 10/50 and 50/50 are defined to represent 2, 10 and 50% probabilities of exceedance in 50 years, respectively. The criteria applied have resulted the number of available records, but it should be mentioned that some each bin does not return the same number of available records. For instance, records which are recorded on soft soil and farm field consist of more than 60% of the record pool, thus the rest is shared between three different groups which are far field – firm soil, near field – soft soil, and near field – firm soil. As a result, selection criteria have to be loosened in some cases.

The scale factors are set such that average of 20 records does not go below the target spectrum in certain percentages and most of the cases the average spectrum is not allowed to go below the target spectrum at all. Similarly, the average spectrum is not allowed to go above 30% of the target spectrum in any point within the period window. In order to control the difference of the positive and negative peaks, where positive peaks refer to the peaks above the target spectrum and vice versa, another criterion is also applied to check the individual records. According to this, the individual record is not allowed to go below the target spectrum less than 50%, or above more than 200-300% in any of the peaks. This criterion dictates to select rather smooth records with less peaks, however it is a very harsh criterion to be satisfied. The scale factors in overall are not allowed to be below 0.5 and above 2 in any of the selected records so that the energy content can be controlled.

Two more criteria have been applied to control the energy content, one is the PGV and the other is the Arias Intensity. The purpose of the inclusion of these two criteria is to decrease the scatter, i.e. record-to-record variability of the selected records. In order to do so, a record that fits the target spectrum with the least error has been assigned as the best record, and the selected records are not allowed to have PGV or Arias Intensity values above or below certain ratios as compared to those obtained from the best record. The limits for these criteria had be set so high in some of the bins that they were practically not much effective because the number of available records was already low even without these criteria. Generally, the selected

records are not allowed to have PGV and Arias ıntensity values, after scale factors are applied, above 1/0.6 – 1/0.7 and below 0.6-0.7 of that of the best record.

The selection of records has been done by using acceleration spectra, however similar procedures may and should be produced for velocity and displacement spectra as well. As an example, acceleration spectra and displacement spectra are given Fig. 5. Please note that the differences among the selected records are much higher in displacement spectra when long-period structures are considered, such as the single-story precast structures as presented here.

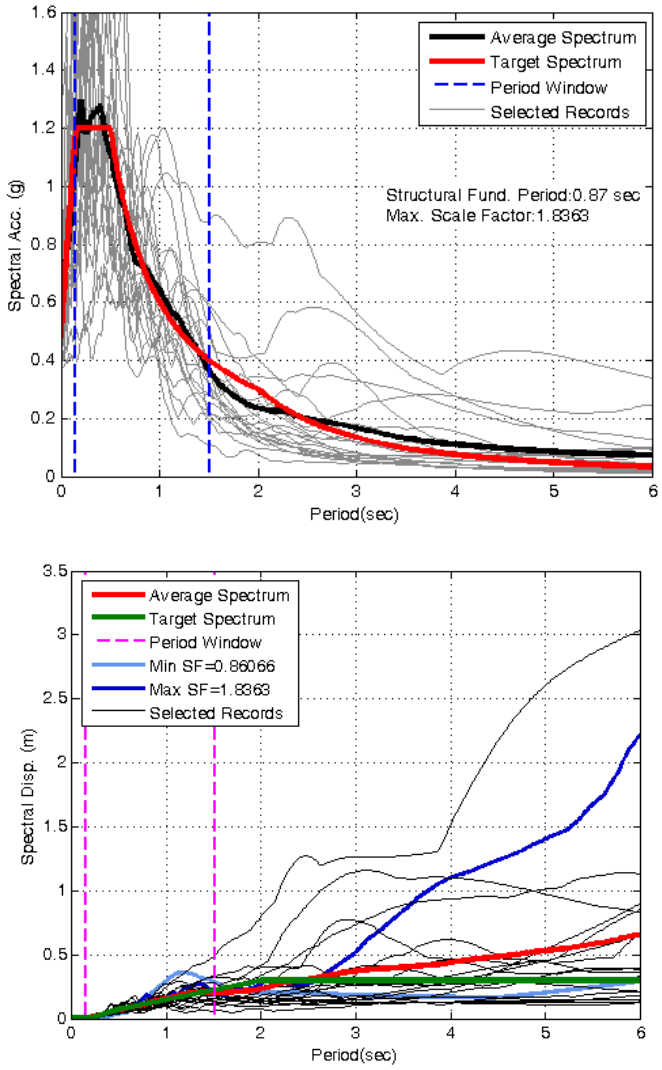

Fig. 5 Acceleration spectra and displacement spectra for an example selection

5 PROPOSED ALGORITHM

The following steps are identified in the proposed algorithm; see the flow chart given in Fig. 6 a,b &c and illustrative description presented in Fig. 7:

- It is assumed that the preliminary design of the structure has been completed so that all requirements in the selected seismic code have been satisfied such as strength and displacement limitations etc. There is no need to discuss what should be initial

stiffness or what is the most suitable lateral load reduction factor or the displacement equality principal is valid or not.

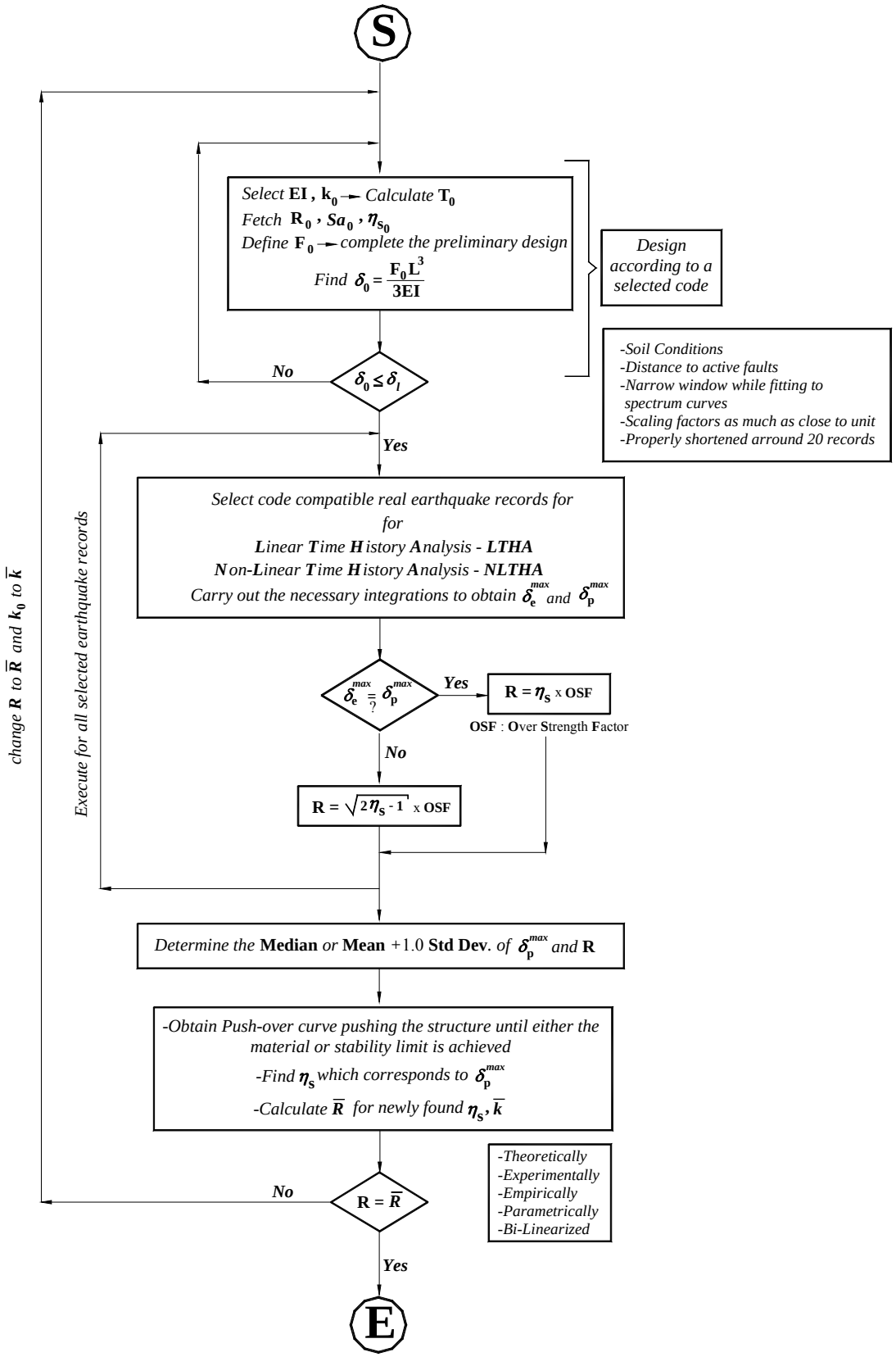

Fig. 6,a - Flow chart of the proposed algorithm : first stage

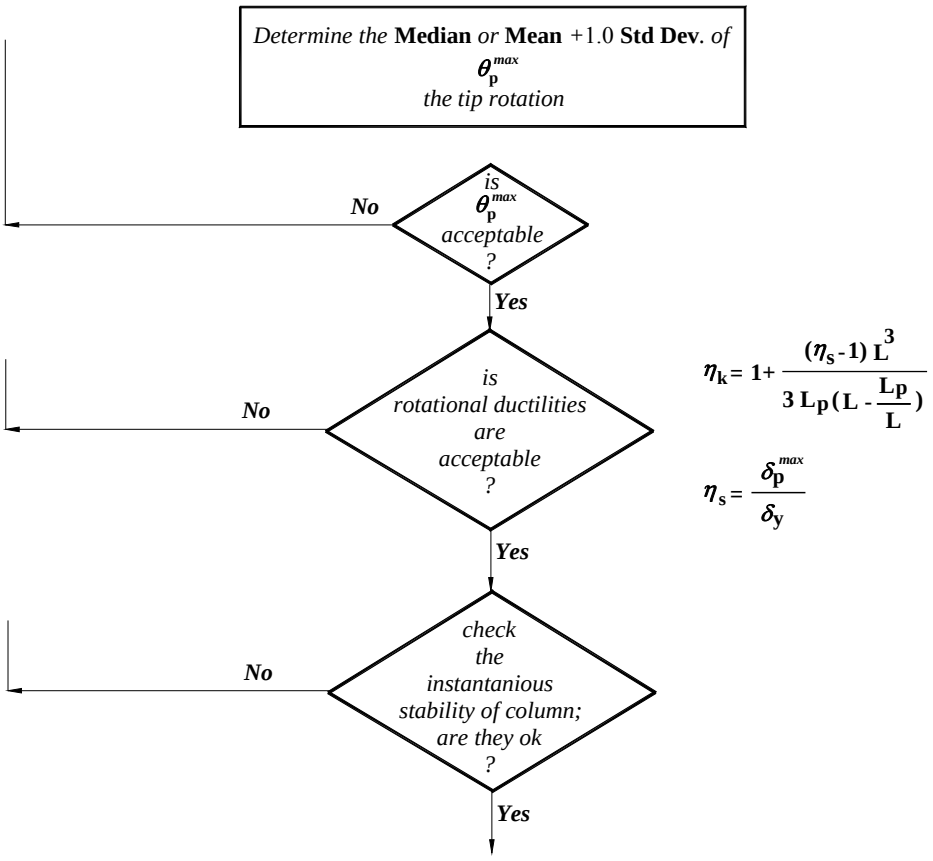

Fig. 6, b - Flow chart of the proposed algorithm: second stage

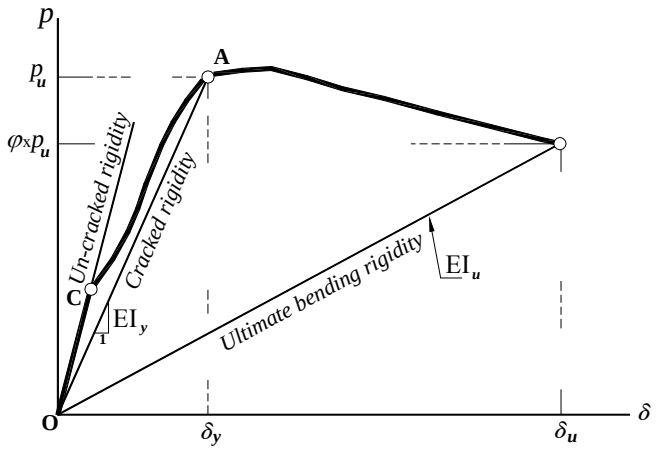

Fig. 6, c – Un-cracked, cracked and ultimate bending rigidities

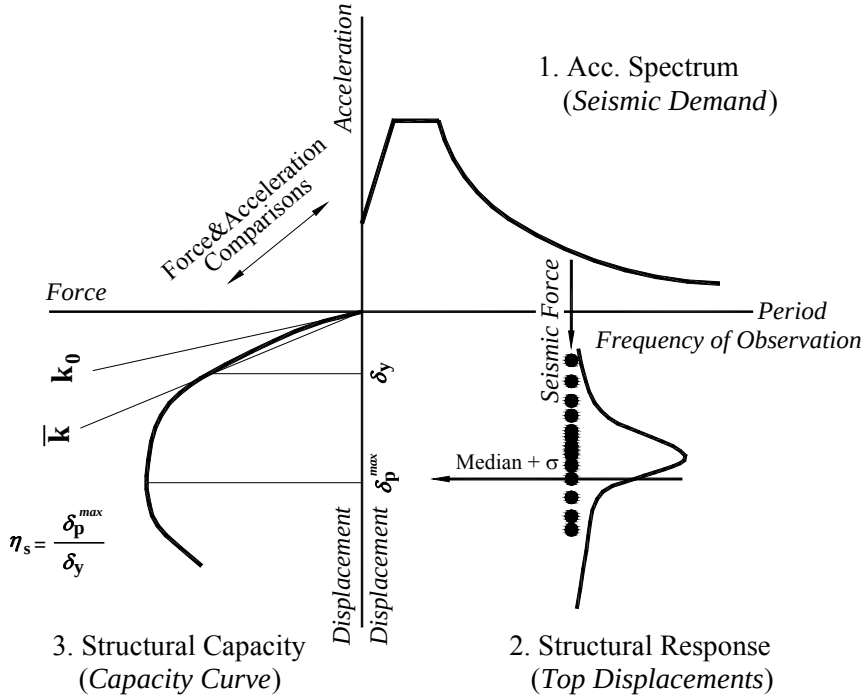

Fig. 7 Description of the proposed procedure

- Real earthquake records are selected so that the parameters like soil conditions, distance to active faults, and the required intensities such as 2/50-10/50-50/50 are all satisfied with reasonable tolerances and scaling factors are chosen as much as close to unity to make the acceleration curves close to the curve provided by codes in a narrowest window around the fundamental period of the structure. The selected earthquakes should be around 20 and the most meaningful part of the records should be identified to shorten the NLTHA analysis which will be used for all records. The details of this topic is discussed below in another sub section.
- The selected partially code compatible earthquakes are used for linear and non-linear analysis of the structure to check which one of the *displacement or energy equality assumption* is valid for the specific structure under consideration. It is also important to have an idea about what could be the tolerance to accept the validity of one of these equalities.
- Depending on the decision done at the end of last step one can calculate the lateral load reduction factor accordingly using the proper formula given in the flow chart.
- Mean plus one standard deviation of maximum displacement obtained through NLTHA and lateral load reduction factors are calculated.
- Capacity curve of the structure is obtained using any one of the known technique. These curves cannot be only obtained theoretically but also experimentally, empirically, parametrically, they can be in a continuous form or in the bilinear form etc.
- Yielding point and the point corresponds to maximum inelastic displacement found are taken into consideration for defining the *lateral rigidity* and the *achieved displacement ductility* of the structure from where the more realistic lateral load reduction factors will be calculated referring to the same formula used in the previous step.

- It is expected to have almost equal lateral load reduction factors in last two cycles of iterations. If they are not at the close proximity then another step of iteration will be carried out.

This will be the end of first stage justification of design. In fact *tip rotations, rotational ductility capacity of critical bottom sections* where the plastic deformations are accumulated and *possible loss of safety against overall and local stability of columns* should be checked as it is proposed in the second stage of the justification process presented in Fig 6,b.

The expected rotational ductility of the critical section can simply and roughly be given as follows [13] for symmetrically reinforced rectangular sections,

$$\mu_k \cong 227 \times \left(\frac{\varepsilon_{cu}}{n} \right)$$

where ε_{cu} and n indicate the maximum concrete strain in uppermost concrete fiber and the dimensionless axial load, $N/(b \times h \times f_{ck})$ respectively. For the derivation of formula presented above it has been assumed that not only the reinforcement bars under tension but the reinforcement bars under compression both are yielded and f_{yk} is around 420 MPa.

The theory which covers the second order effect of axial force on the tip rotation which is significantly different than chord rotation, the tip displacement is summarized in Appendix - 1 together with the overall stability criterion of column considering the material nonlinearity exist in the critical region. The material nonlinearity is simply imparted into the second order analysis by means of the decrements in bending rigidities shown in Fig.6 c. Numerical examples indicate that especially the loss of overall stability of the column cannot be neglected and the excessive tip rotations may become a good reason to destabilize the roof beams sitting on the columns.

In the following paragraphs several definitions and explanations are given and some complementary results of early experimental and theoretical findings for *over strength factor, lateral load reduction factors and capacity curves* are summarized for the sake of having complete information together with this justification procedure.

6 OVER STRENGTH AND LATERAL LOAD REDUCTION FACTORS

For the sake of completeness the early results achieved by reviewing the experimentally obtained and theoretically examined column behavior has been added into this paragraph [9,10].

The 4.0 m high column having a cross section of 40×40 cm, Fig. 8a, subjected to displacement reversals exposed the structural response shown in Fig. 8b. The same hysteresis loops have been obtained theoretically and compared in Fig. 8c with the experimental results. Then the material coefficients have been reduced from 1.15 and 1.4 to unity for steel and concrete respectively before the similar theoretical works carried out. The envelope of hysteresis curves are compared in Fig. 8d.

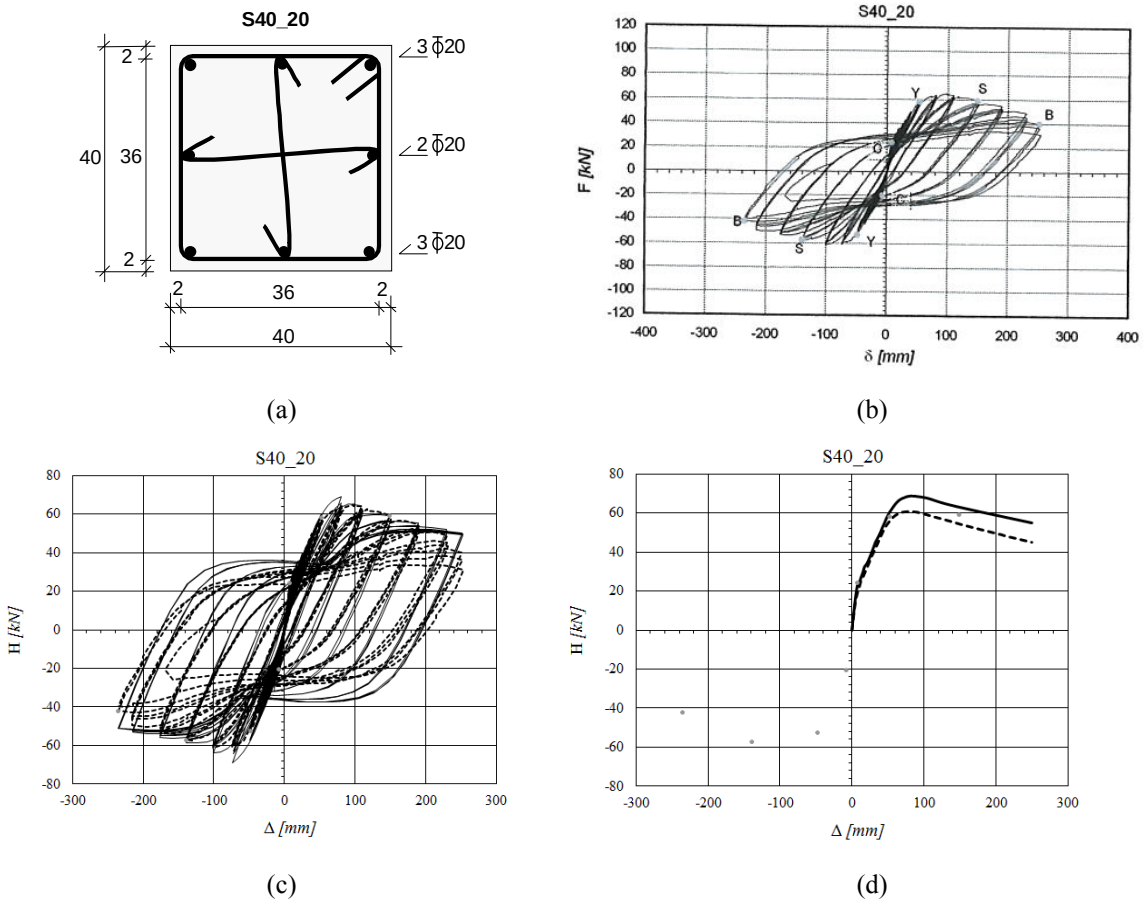

Fig. 8 Experimental and analytical evaluation of 40×40 cm column

Similar 12 more tests have been completed and similar analyses have been carried out depending on the results obtained and Table 1 is prepared, [10]. One can found the ultimate loads of the columns when the material coefficient is taken as unity or different than unity, in the first two lines, respectively. The ratio of these two lines give the approximate over-strength factors. It can be concluded that for these type of columns the over-strength factors can be taken as 1.10. If the displacement ductilities obtained from the same tests which are given in the fourth line of Table 1 are multiplied by over strength factor the lateral load reduction factors on the fifth line will be achieved.

SPECIMEN	1	2	3	4	5	6	7	8	9	10	11	12	13
	S30_14	S30_14M	S30_16	S30_18	S30_18Z	S35_1416	S35_18	S35_20	S35_20Z	S40_16	S40_20	S40_2020	S40_2020Z
$P_{u\,(\gamma=1)}$	21.30	21.00	29.10	32.60	30.40	33.50	42.50	50.40	48.00	49.30	68.50	88.30	89.76
$P_{u\,(\gamma\neq1)}$	19.00	19.50	25.20	28.60	26.80	29.70	37.70	44.30	42.20	43.70	60.70	77.73	77.40
OSF	1.12	1.08	1.15	1.14	1.13	1.13	1.13	1.14	1.14	1.13	1.13	1.14	1.16
μ	5.30	3.20	5.10	3.70	3.00	5.80	5.50	4.60	3.90	5.20	5.50	3.00	3.40
OSF × μ	5.94	3.44	5.89	4.22	3.40	6.54	6.20	5.23	4.44	5.87	6.21	3.41	3.94

Table 1 Overstrength factors, displacement ductility ratios and possible lateral load reduction factors

7 CAPACITY CURVES

Capacity curves used in the above explained algorithm can be obtained either by means of a theoretical manner or it can be obtained by any one of the known simplified technique. They can be in a continuous form or in bi-linear form.

Sometimes for the same size same quality concrete but for different reinforcement ratios simple ready charts can be utilized for that purpose. An example of a capacity curve for 30×30 cm C25 square column obtained experimentally, theoretically and parametrically is presented in Fig. 9, as well, [9].

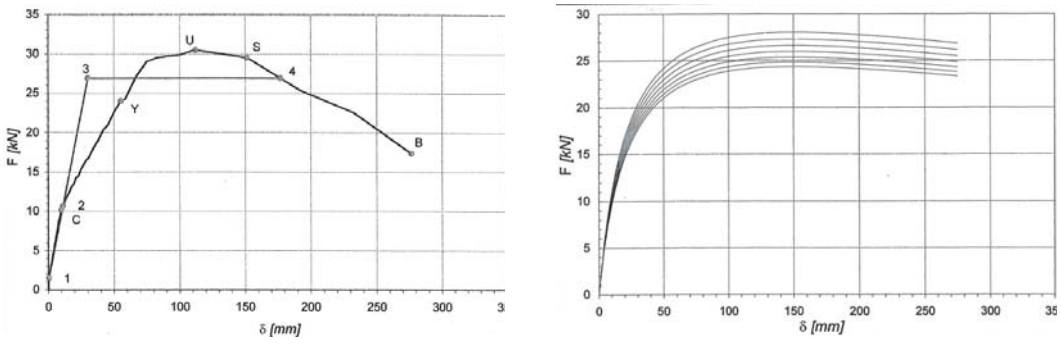

(a) (b)

Fig. 9 Determination of the column capacity curve

8 NUMERICAL EXAMPLES

The presented algorithm has been used to make clear the following issues;

- To what extent the assumptions made at the beginning of preliminary design are satisfied? Namely, have the strength, the lateral load reduction factor and /or the displacement ductility assumptions as well as the stiffness values used in design been checked?
- The design is accepted when one or several of parameters are satisfied. What are the tolerance limits for satisfaction of the design criteria?

The initial design parameters and the findings are presented for three columns, Column #1 to #3. The Column #1 is extracted from the benchmark structure of Safecast Project, [14]. Column # 2 is one of the prefabricated columns tested at ITU laboratories [9]. The Column # 3 is extracted from a real structure currently in use in Kocaeli, Turkey.

The algorithm proposed above was run for each of the columns mentioned here. The algorithm has converged in three steps for all columns. The results as well as the key parameters per each analysis step have been presented in Table 2.

The results presented in Table 2 are based on the assumption that the change of R factor in two consecutive steps will not exceed a tolerance, which is 10% in this study. This tolerance as well as tolerance limits of other parameters may be adjusted by the user depending on parametric studies and findings.

Parameter	Unit	Soil Type B 60×60 Column	Soil Type C 40×40 Column	Soil Type B 70×70 Column
m	tonnes	33	20.4	43.4
K_0	kN/m	2230	1946	582.1
T_0	sec	0.75	0.64	1.54
$Sa(T=T_0)$	g	0.61	0.95	0.34
R		3	3	3
F_{design}	kN	65.80	63.40	36.70
K_1	kN/m	1453	829	349
T_1 (yield)	sec	0.93	0.98	1.99
Sa ($T=T_1$)	g	0.51	0.66	0.28
R_1		2.26	2.02	1.97
$\lvert(R_1-R_0)/R_0\rvert$	>10%	0.25	0.33	0.34
F_{design} (m+s)	kN	73.10	65.40	60.60
K_2	kN/m	1671	1129	379
T_1 (yield)	sec	0.87	0.84	1.91
Sa ($T=T_1$)	g	0.54	0.76	0.29
R_2		2.43	2.05	2.14
$\lvert(R_2-R_1)/R_1\rvert$	OK	0.08	0.01	0.09
F_{design} (m+s)	kN	71.90	74.20	57.70

Table 2 Progress of the algorithm and the change of key design parameters for the case study columns

Comparison of the assumed capacity curve with the pushover and time history analyses results for columns are presented in Figs. 10, 11 and 12.

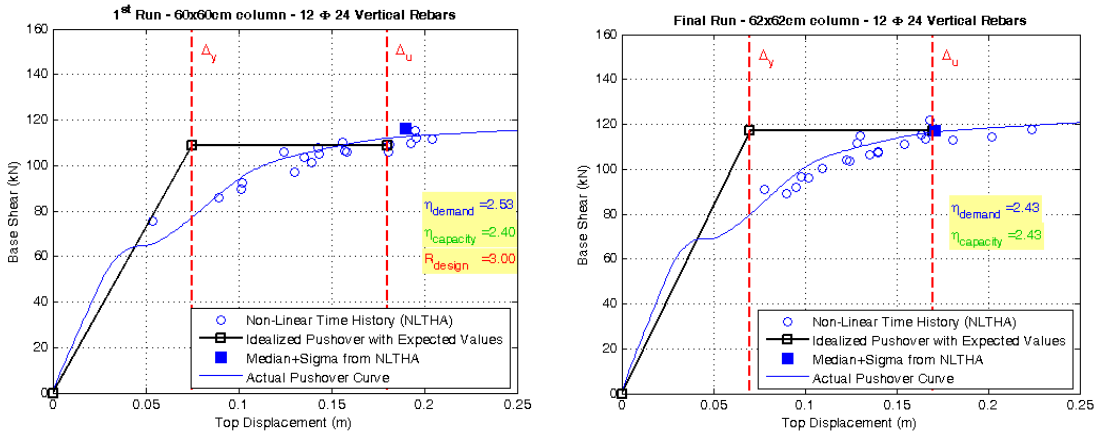

Fig. 10 Comparison of the assumed capacity curve with the pushover and time history analyses results for the **Column #1**

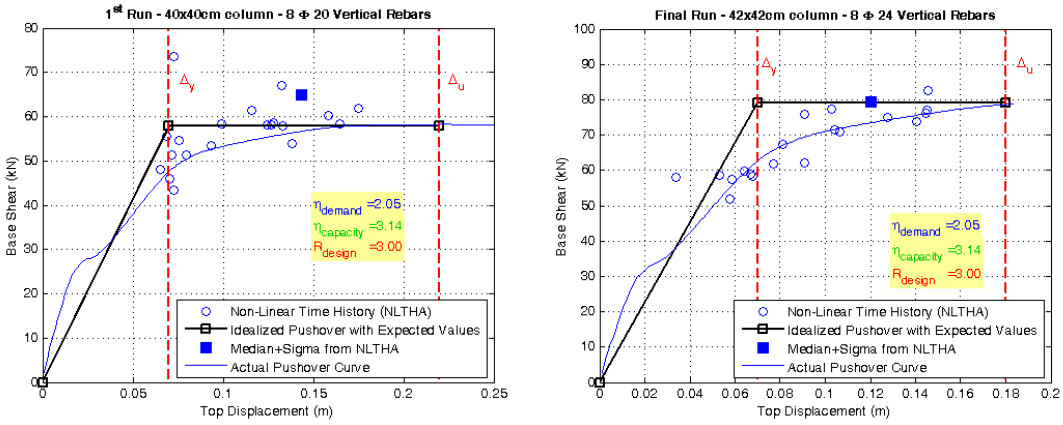

Fig. 11 Comparison of the assumed capacity curve with the pushover and time history analyses results for the **Column #2**

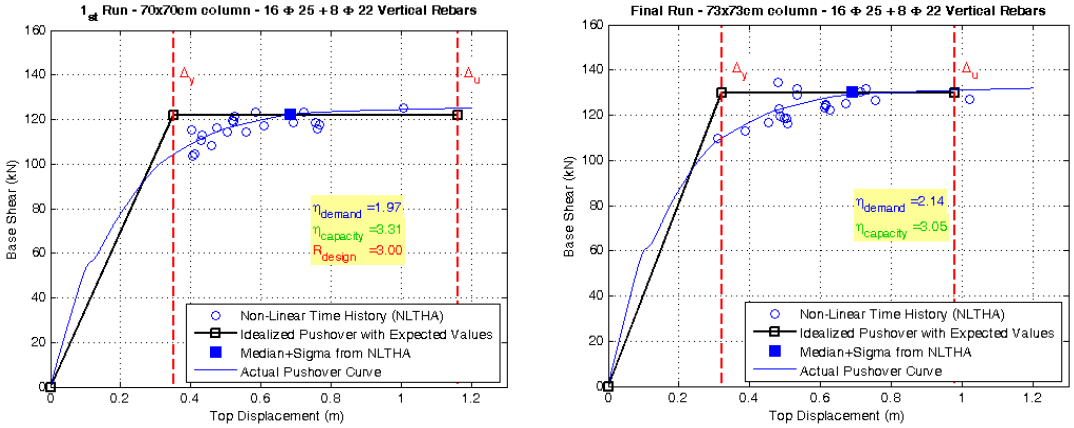

Fig. 12 Comparison of the assumed capacity curve with the pushover and time history analyses results for the **Column #3**

The results presented in Figs. 10, 11 and 12 are representative of all possible cases in design iterations when the proposed algorithm is used. In the first example, the displacement condition is not satisfied (i.e. the displacement demand of the original column is higher than the displacement capacity of the structure). The strength is not satisfied in the second example. The third example satisfies both conditions but the algorithm was still run in order to see how the design would change. It can be observed in these figures that the column dimensions and/or reinforcement need to be changed in all cases in order to satisfy the design algorithm proposed here.

Please note that the scale factors for some of the records listed in Table 3 are higher than 2. These are the cases where the number of available records for the set of criteria used was not high thus the scale factor condition was loosened.

One of the key points of the algorithm proposed here, which is also one of the main motivations of the study, is that the spectral displacement equality (i.e. equal displacement rule) which is the basis of the conventional design is not valid in most of the cases. The analyses show that for the examined three columns, the average plastic displacements calculated by applying selected 20 records on the columns is always higher than the spectral displacements found from the displacement spectra of the selected records. In other words, the equal displacement rule certainly does not work for the cases examined.

60×60 cm Column		40×40 cm Column		70×70 cm Column	
Record	**SF**	**Record**	**SF**	**Record**	**SF**
CHICHI03_TCU129-E	**1.25**	CHICHI06_TCU078-E	**1.31**	CHICHI03_TCU122-E	**2.42**
HECTOR_HEC090	**0.98**	CHICHI03_TCU129-E	**0.99**	CHICHI_TCU136-W	**2.16**
CHICHI_TCU047-N	**1.25**	CHICHI_CHY046-N	**1.58**	CHICHI_TCU128-N	**1.57**
CHICHI_CHY035-N	**0.96**	BIGBEAR_DHP090	**1.44**	CHICHI_TCU116-N	**1.83**
CHICHI_CHY034-W	**0.90**	MORGAN_G06090	**0.97**	CHICHI_TCU106-N	**1.74**
NORTHR_PKC360	**0.86**	HECTOR_HEC000	**1.47**	CHICHI_TCU087-N	**2.15**
NORTHR_STN110	**1.03**	CHICHI_TCU-E	**1.32**	CHICHI_TCU063-N	**1.35**
NORTHR_PEL360	**1.28**	CHICHI_CHY074-E	**1.36**	CHICHI_TCU054-N	**1.97**
LOMAP_G03090	**1.22**	CHICHI_ALS-E	**1.43**	CHICHI_TCU039-N	**1.85**
LOMAP_CYC285	**1.04**	NORTHR_PKC090	**0.91**	CHICHI_TCU029-N	**1.77**
CHICHI_TCU138-N	**1.04**	NORTHR_MRP090	**1.53**	CHICHI_CHY029-N	**1.73**
CHICHI_TCU116-E	**1.24**	NORTHR_0141-270	**1.01**	CHICHI_TCU136-N	**1.99**
CHICHI_TCU063-E	**1.26**	LANDERS_MVH000	**1.45**	CHICHI_TCU107-E	**1.75**
CHICHI_TCU047-E	**0.91**	LOMAP_SLC270	**1.27**	CHICHI_TCU082-E	**1.96**
CHICHI_TCU045-E	**1.19**	WHITTIER_A-CAS000	**1.09**	CHICHI_TCU054-E	**2.39**
CHICHI_CHY024-E	**1.28**	WESTMORL_PTS225	**1.49**	CHICHI_TCU039-E	**1.72**
NORTHR_PKC090	**1.04**	CORINTH_COR--L	**1.33**	CHICHI_TCU-E	**2.04**
NORTHR_LOS000	**0.99**	VICT_CPE045	**0.8**	CHICHI_CHY074-E	**1.78**
LOMAP_STG000	**1.04**	TABAS_DAY-LN	**1.58**	CHICHI_ALS-E	**1.92**
VICT_CPE045	**0.93**	FRIULI_A-TMZ000	**1.45**	KOBE_KBU000	**1.31**

Table 3 Selected earthquake records and scale factors (SF)

The displacement equality is the base of the conventional design because the behavior factor, R, is the most important assumption of the conventional design. A graphical description of the terms and the design assumption are presented in Fig. 13.

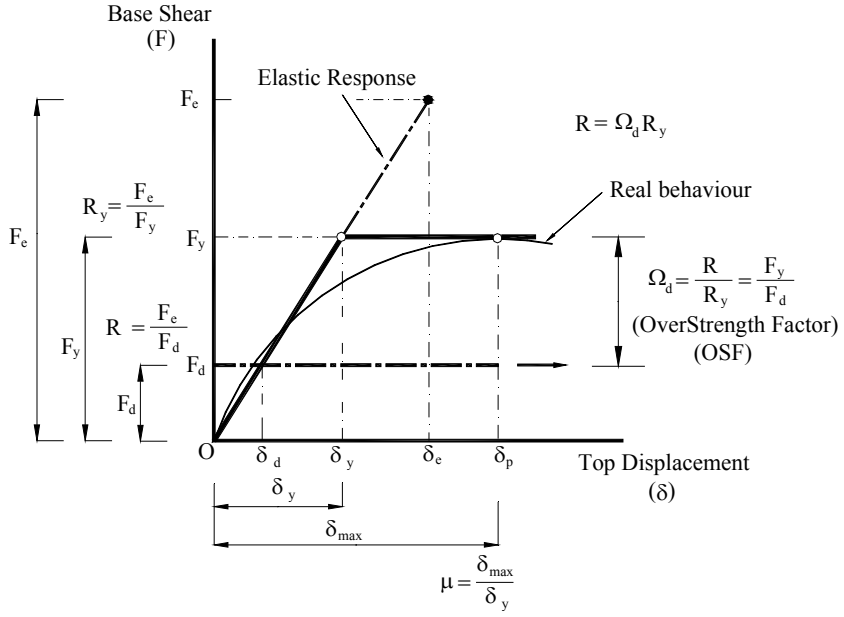

Fig. 13 The use of equal displacement rule in design

The results shown in Fig. 14 indicate a significant disagreement between the spectral and real displacement demands. Please note that the period of the three columns presented in the

plot shown in Fig. 14, columns of 40×40, 60×60 and 70×70, are 0.64 sec, 0.75 sec and 1.54 sec, respectively. As it can be seen in Fig. 14, as the period of the system increases, the disagreement becomes even more evident.

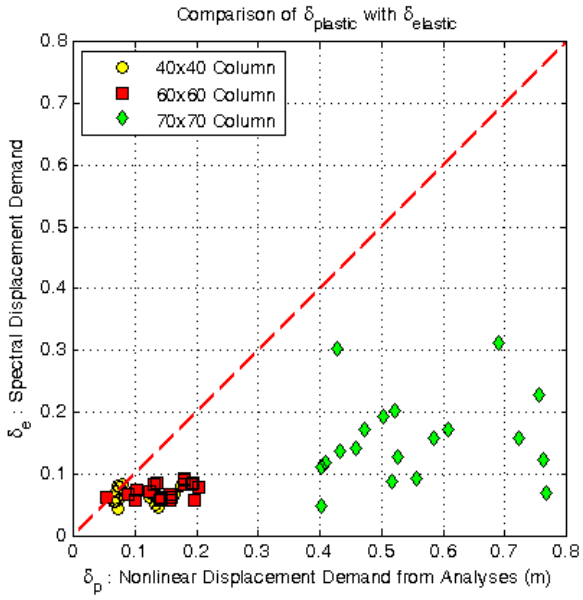

Fig. 14 Comparison of the elastic spectral displacements with the plastic displacement demands obtained from the nonlinear dynamic analyses

The stability analyses of one of the columns have been examined in Table 4. In the analysis, three critical stages namely un-cracked, yielding and ultimate state have been accounted. The equations presented in Appendix I are utilized for the stability analysis. It can be considered that the stability check of a column in the different stages of nonlinear phase is an essential matter.

			40 x 40 Column (L=4.00m) - Stability Checks			
	Lateral Stiffness [kN/m]		Buckling Load [kN]		Buckling Length [m]	
			Fixed Based	Partially Fixed	Fixed Based	Partially Fixed
Un-Cracked	K_0	1946	6394	6394 (γ=0)	8.00	8.00 (γ=0)
Yielding	K_y	829	2724	1185	8.00	12.19 (γ=0.581)
Ultimate	K_u	264	867	162	8.00	18.56 (γ=1.838)

Table 4 Stability analyses of Column 40×40 cm

9 CONCLUSIONS

The following conclusions are drawn:

- Design verification is needed and if necessary redesign step of iterations are carried out.
- It is possible to overcome the inherently existing deficiencies of spectrum based design by the algorithm presented; namely the strength and stiffness degradations and

time duration effects can be considered which are not considered in the code specified spectrum analyses. In this technique, at the beginning of design stage, there is no need to make a series of assumptions such as the initial stiffness of the structure, displacement ductility of the structure and lateral load reduction factor which are all effective on the results. It becomes possible to trace the actual behavior of structure during the iteration steps.

- The top displacements obtained by NLTHA which are based on nearly code compatible real earthquake records are generally bigger than code limits and they are practically not equal to the elastic displacements obtained by linear time history analyses. Therefore the widely utilized assumption of *displacement equality* cannot be generalized for the columns analyzed and *equality of velocities* or *energies* should be considered wherever is needed. The algorithm presented here is providing a versatile tool for that purpose.
- The proposed procedure can be used not only for single story precast buildings but it can be generalized by minor alterations for the design of bridge columns or piers and for the critical columns of piloty type building structures where all the nonlinear behavior is observed only in one of the generally lower stories.
- The execution time for nonlinear time history analyses needed in the proposed algorithm is not a big issue because of the speed reached by computers but more discussions should be done on the selection of real records and their optimal numbers.

- Several more checks has been added to the flow chart presented in [15] to have more refined one for controlling the sufficiency of sectional ductility needed to provide the required displacement ductility and to check the allowable tip rotations to keep the top beams stable in their original position and check for the overall stability of the columns. The algorithm proposed may be supported depending on new research in the field of defining reasonable limits for tip rotations and loss of safety against overall stability of the structure.

10 REFERENCES

[1] Saatcioglu M., Mitchell D., Tinawi R., Gardner N.J., Gillies A.G., Ghobarah A., et al. "The August 17, 1999, Kocaeli (Turkey) Earthquake – Damage to Structures", *Can J Civ Eng* 28: 715-37, 2001.

[2] Ataköy H., "17 August Marmara Earthquake and the Precast Structures Built by TPCA Members", *Turkish Precast Concrete Association*, Ankara, Turkey, 1999.

[3] Sezen H., Elwood K.J., Whitaker A.S., Mosalam K.M., Wallace J.W., Stanton J.F., "Structural Engineering Reconnaissance of the August 17, 1999, Kocaeli (Izmit), Turkey", Earthquake Rep No 2000/09. Pacific Engineering Research Center. University of California, Berkeley, CA, 2000.

[4] Bruneau M., "Building Damage from the Marmara, Turkey Earthquake of August 17, 1999", *J Seismo* 6(3): 357-77, 2002.

[5] Sezen H., Whittaker A.S., "Seismic Performance of Industrial Facilities Affected by the 1999 Turkey Earthquake", *J Per Const Fac* ASCE 20(1): 28-36, 2006.

[6] Wood S.L., "Seismic Rehabilitation of Low-Rise Precast Industrial buildings in Turkey", In: Wasti T, Ozcebe G (eds), *Advances in Earthquake Engineering for Urban Risk*

Reduction. NATO Science Series. IV. Earth and Environmental Sciences: Kluwer Academic Publishers 66: 167-77, 2003.

[7] Karadogan F., "Prefabricated Industrial Type Structures of Adapazarı", *Irregular Structures*, European Association of Earthquake Engineering, Task Group 8, Asymmetric and Irregular Structures, Istanbul, Vol. 2, October 1999.

[8] Karadogan F., Yuksel E., Ilki A., "Deformability Limits and Ductility of Reinforced Concrete Bare Frames", *First Japan – Turkey Workshop on Earthquake Engineering*, Istanbul, Vol.1, March 1997.

[9] Karadogan F., Yuksel E., Yuce S., Taskın K., Saruhan H., "Experimental Study on the Original and Retrofitted Precast Columns", Technical Report (in Turkish), Istanbul Technical University, 2006.

[10] Karadogan, F., Yuce, S., Yuksel, E., Bal, I.E., Hasel, F.B., "Single Story Precast Structures in Seismic Zones-I", COMPDYN 2013, 4th ECCOMAS Thematic Conference on Computational Methods in Structural Dynamics and Earthquake Engineering, Kos Island, Greece, 12–14 June 2013.

[11] PEER NGA Database. Pacific earthquake engineering research center: NGA database. (http://peer.berkeley.edu/peer_ground_motion_database/)

[12] http://web.itu.edu.tr/~iebal/Dr_Ihsan_Engin_BAL/SafeCladding_EU_Project.html

[13] Çakıroğlu A., Karadoğan F., "Plastic Hinge Capacities, Curvature and Structural Ductilities of RC Structures", First Japan-Turkey Workshop on Earthquake Engineering, March, 1997, Istanbul, Vol I.

[14] SAFECAST FP7 Project "Performance of innovative mechanical connections in precast building structures under seismic conditions", Coordinated by Dr. Antonella Colombo.

[15] Karadogan, F., "An algorithm to justify the design of single storey precast structures", Theme Lecture, Second European Conference on Earthquake Engineering, 2ECEES 2014, Istanbul.

[16] Karadogan F., Pala S., Yuksel E., Durgun Y., "Yapı Mühendisliğine Giriş Yapısal Çözümleme Cilt III Hiperstatik Sistemler Yerdeğiştirme Yöntemleri", Istanbul, 2015, *in Turkish.*

[17] Çakıroğlu A., "Kayma Şekildeğiştirmeleri Gözönünde Tutulan II.Mertebe Teorisine Ait Çubuk Sabitleri, Teknik Rapor No: 32, 1978, Istanbul, *in Turkish.*

APPENDIX I

Second order effect of axial force on tip rotation and tip displacement and the stability of column with plastic deformations in critical zone

The plastic deformations of a column subjected to conservative axial force and lateral load reversals are accumulated generally slightly above the bottom critical sections. This is a realistic assumption to simplify the design and its justification. It is possible to obtain the exact tip rotation and tip deflection of a semi rigid supported column or a pier which is subjected to single moment M or single lateral load P on top, according to the second order theory without omitting the shear deformations which may accompany with flexural deformations see Fig. A

a&b and Fig. B. It will be assumed that the flexural EI, and shear GF', rigidities of the column are both constant along the height of the element. Since the stiffness coefficients of such a member can be derived easily, the case with variable EI and/or GF' can be handled easily as well [15,16, 17].

The following paragraphs not only outlines the derived necessary equations for tip rotations and tip displacements for several cases but also include the characteristic equation for the stability of the element.

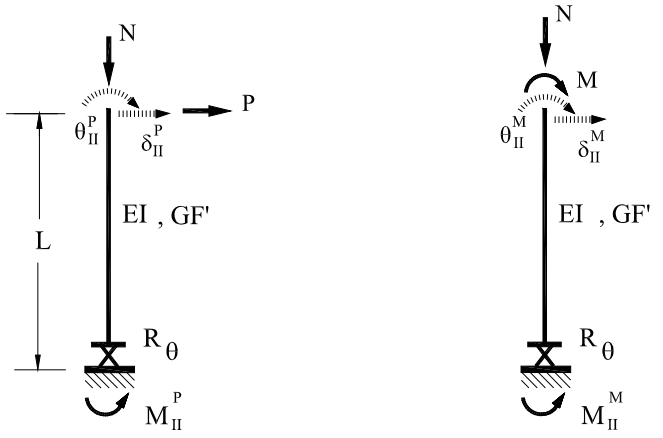

a- Lateral single load on top **b - Single moment on top**

Fig. A

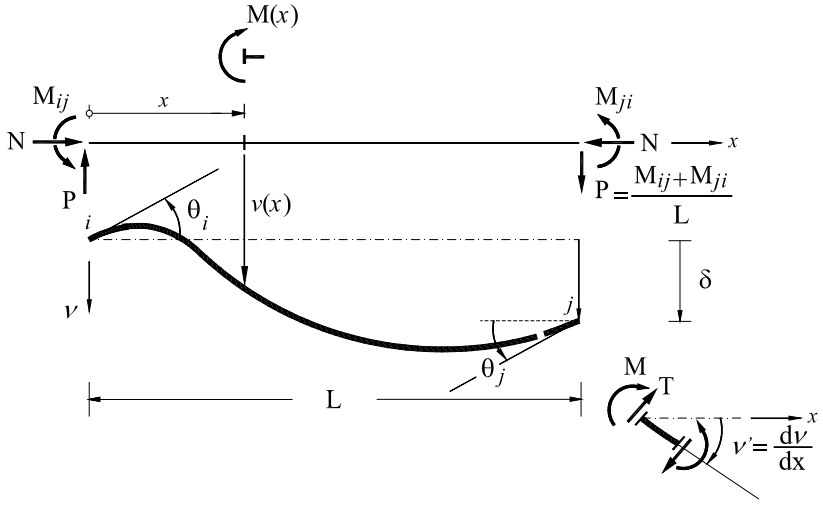

Fig. B

i- General abbreviations and differential equilibrium equation of the problem

$$EI^* = EI \times \left(1 - \frac{N}{GF'}\right) \quad , \quad \left(1 - \frac{N}{GF'}\right) = 1 - \beta \times (\alpha L)^2 \quad , \quad \beta = \frac{EI}{L^2 GF'} \quad , \quad \gamma = \frac{EI}{L\,R_\theta}$$

$$\alpha L = L \times \sqrt{\frac{N}{EI}} \quad , \quad \bar{\alpha} L = L \times \sqrt{\frac{N}{EI^*}} = \alpha L \times \sqrt{\frac{1}{1 - (\alpha L)^2 \times \beta}}$$

$$\bar{R}_\theta = R_\theta \times (1 - \frac{N}{GF'})$$

Subscripts I and II are referring to first and second order theories respectively

$$M(x) = -\left(M_{ij}\right) + \left(\frac{M_{ij} + M_{ji}}{L}\right)x + |N| \times \nu(x) \quad , \quad P = \left(\frac{M_{ij} + M_{ji}}{L}\right)$$

$$\frac{d^2\nu(x)}{dx^2} + \frac{M(x)}{EI^*} = 0 \;\Rightarrow\; \nu''(x) + \bar{\alpha}^2 \times \nu(x) = \left(\frac{M_{ij}}{EI^*}\right) - \left(\frac{P}{EI^*}\right)x$$

$$\nu(x) = C_1 \sin\bar{\alpha}x + C_2 \cos\bar{\alpha}x + \left(\frac{M_{ij}}{|N|}\right) - \left(\frac{P}{|N|}\right)x$$

ii- Single concentrated lateral load P on top together with a conservative single axial load N, Fig Aa

General solution of differential equation and the boundary conditions

$$\nu(x) = C_1 \sin\bar{\alpha}x + C_2 \cos\bar{\alpha}x + \left(\frac{M_{ij}}{\bar{\alpha}^2 \times EI^*}\right) - \left(\frac{P}{\bar{\alpha}^2 \times EI^*}\right)x \tag{1}$$

$$\nu(0) = 0 \quad , \quad \left(\frac{d\nu}{dx}\right)_{x=0} = \frac{M_{ij}}{\bar{R}_\theta} + \frac{P}{GF' \times (1 - \frac{N}{GF'})} \tag{2a}$$

and the constants C_1 and C_2 becomes

$$C_1 = \left(\frac{P}{\bar{\alpha}^2 \times EI^*}\right) + \left(\frac{M_{ij}}{\bar{\alpha} \times \bar{R}_\theta}\right) + \left(\frac{P}{\bar{\alpha} \times GF' \times (1 - \frac{N}{GF'})}\right), \quad C_2 = -\left(\frac{M_{ij}}{\bar{\alpha}^2 \times EI^*}\right) \tag{2b}$$

Hence the general expresssion for *displacements* will be obtained as follows

$$\nu(x) = \left(\frac{P}{\bar{\alpha}^2 \times EI^*} + \frac{M_{ij}}{\bar{\alpha} \times \bar{R}_\theta} + \frac{P}{\bar{\alpha} \times GF' \times (1 - \frac{N}{GF'})}\right)\sin\bar{\alpha}x - \left(\frac{M_{ij}}{\bar{\alpha}^2 \times EI^*}\right)\cos\bar{\alpha}x + \left(\frac{M_{ij}}{\bar{\alpha}^2 \times EI^*}\right) - \left(\frac{P}{\bar{\alpha}^2 \times EI^*}\right)x \tag{3}$$

The bending moment at the critical bottom section can be determined simply by moment equilibrium equation written down considering the deformed shape of the column

$$M_{II}^{(P)} = P \times L + N \times \nu(L) = M_I^{(P)} + N \times \nu(L) \tag{4a}$$

where $M_I^{(P)} = P \times L$

If it is required Equation (4a) can be rearranged in terms of the following definition

$$\varphi^{(P)} = \left(\frac{1 + \beta \times (\bar{\alpha}L)^2}{\cos\bar{\alpha}L - \gamma \times (\bar{\alpha}L) \times \sin\bar{\alpha}L} \times \frac{\sin\bar{\alpha}L}{(\bar{\alpha}L)}\right)$$

$$M_{II}^{(P)} = M_I^{(P)} \times \varphi^{(P)} \tag{4b}$$

The tip displacement $\delta_{II}^{(P)}$ can be extracted from the following equilibrium equation

$$M_{II}^{(P)} = M_I^{(P)} + N \times \delta_{II}^{(P)}$$

as

$$\delta_{II}^{(P)} = \frac{\left(M_{II}^{(P)} - M_I^{(P)}\right)}{N} \tag{5}$$

If Eq. (4b) is used in Eq.5 then $\delta_{II}^{(P)}$ will be

$$\delta_{II}^{(P)} = M_I^{(P)} \times \frac{L^2}{EI^*} \times \frac{1}{(\bar{\alpha}L)^2}(\varphi^{(P)} - 1) \tag{5a}$$

obtained.

The first derivative of the Eq.(3) at $x=L$ will be the required tip rotation according to the second order theory :

$$\theta_{II}^{(P)} = P\left(\frac{\cos\bar{\alpha}L}{GF'} + \frac{\cos\bar{\alpha}L - 1}{\bar{\alpha}^2 \times EI^*}\right) + M_{II}^{(P)}\left(\frac{\cos\bar{\alpha}L}{\bar{R}_\theta} + \frac{\sin\bar{\alpha}L}{\bar{\alpha} \times EI^*}\right) \tag{6}$$

iii- Single concentrated moment M on top together with a concervative single axial load N, Fig A.b

The general solution of the equilibrium equation written according to the second order theory is as follows

$$v(x) = C_1 \sin\bar{\alpha}x + C_2 \cos\bar{\alpha}x + \left(\frac{M_{ij}}{\bar{\alpha}^2 \times EI^*}\right) \tag{7}$$

and with the boundary conditions given below

$$v(0) = 0 \quad , \quad \left(\frac{dv}{dx}\right)_{x=0} = \frac{M_{ij}}{\bar{R}_\theta} \tag{7a}$$

one can determine the constants C_1 and C_2

$$C_1 = \left(\frac{M_{ij}}{\bar{\alpha} \times \bar{R}_\theta}\right) \quad , \quad C_2 = -\left(\frac{M_{ij}}{\bar{\alpha}^2 \times EI^*}\right) \tag{7b}$$

and hence the following general solution is achieved;

$$v(x) = \left(\frac{M_{ij}}{\bar{\alpha} \times \bar{R}_\theta}\right)\sin\bar{\alpha}x - \left(\frac{M_{ij}}{\bar{\alpha}^2 \times EI^*}\right)\cos\bar{\alpha}x + \left(\frac{M_{ij}}{\bar{\alpha}^2 \times EI^*}\right) \tag{8}$$

The bending moment at the critical section according to the second order theory can be simply derived by the moment equilibrium equation of the column as follows

$$M_{II}^{(M)} = M + N \times v(L) = M_I^{(M)} + N \times v(L) \tag{9a}$$

If the following two definitions are used

$$M_I^{(M)} = M$$

$$\varphi^{(M)} = \left(\frac{1}{\cos\bar{\alpha}L - \gamma \times (\bar{\alpha}L) \times \sin\bar{\alpha}L}\right)$$

then

$$M_{II}^{(M)} = M_{I}^{(M)} \times \varphi^{(M)} \tag{9b}$$

can be written.

For the tip displacement and for the tip rotations $\delta_{II}^{(M)}$ ve $\theta_{II}^{(M)}$ due to the tip monet M one can derive the following two expressions

$$\delta_{II}^{(M)} = M_{I}^{(M)} \times \frac{L^2}{EI^*} \times \frac{(\varphi^{(M)} - 1)}{(\bar{\alpha}L)^2} = M_{I}^{(M)} \times \frac{L^2}{EI \times \left(1 - \frac{N}{GF'}\right)} \times \frac{1}{(\bar{\alpha}L)^2} \left(\frac{1 - \left(\cos \bar{\alpha}L - \gamma \times (\bar{\alpha}L) \times \sin \bar{\alpha}L\right)}{\left(\cos \bar{\alpha}L - \gamma \times (\bar{\alpha}L) \times \sin \bar{\alpha}L\right)} \right) \tag{10}$$

$$\theta_{II}^{(M)} = M_{I}^{(M)} \times \frac{L}{EI \times \left(1 - \frac{N}{GF'}\right)} \times \left(\frac{\gamma \times \cos \bar{\alpha}L + \frac{\sin \bar{\alpha}L}{\bar{\alpha}L}}{\left(\cos \bar{\alpha}L - \gamma \times (\bar{\alpha}L) \times \sin \bar{\alpha}L\right)} \right) \tag{11}$$

It is interesting to note that if the moment which makes the tip rotation $\theta_{II}^{(M)} = 1$ is searched this can be achieved through the Eq.10 as follows

$$\bar{m}_{j_{\theta j}} = \bar{k}_{22} = \frac{EI}{L} \times \left(1 - \frac{N}{GF'}\right) \times \left(\frac{\left(\cos \bar{\alpha}L - \gamma \times (\bar{\alpha}L) \times \sin \bar{\alpha}L\right)}{\gamma \times \cos \bar{\alpha}L + \frac{\sin \bar{\alpha}L}{\bar{\alpha}L}} \right) \tag{12}$$

This is a special *rotational stiffness coefficient* by definition and it is going to be used as the characteristic equation for stability. In other words $\bar{\alpha}L$ which makes zero the Eq. 12 will define the stability load of the column with concentrated plastic deformation at the critical section. It should be kept in mind that the buckling length of the cantilever shown in Fig. C.b may even bigger than two times the height of the column.

When the effect of shear deformation is neglected in Equation 4b, one can reach Equation 13. It is important to review the *chord rotations* and *tip rotations* simply comparing the exact values of them obtained through the above summarized formulations. If once again the column given in Fig. C.a is considered and if

$$\varphi^{(P)} = \left(\frac{1}{\cos \alpha L - \gamma \times (\alpha L) \times \sin \alpha L} \times \frac{\sin \alpha L}{(\alpha L)} \right)$$

is defined then tip displacement and associated *chord rotations* are given as follows

$$\delta_{II}^{(P)} = \frac{PL^3}{EI} \times \frac{1}{(\alpha L)^2} (\varphi^{(P)} - 1) \quad \Rightarrow \quad \theta_{II,chord}^{(P)} = \left(\frac{\delta_{II}^{(P)}}{L} \right) = \left(\frac{PL^2}{EI} \right) \times \frac{1}{(\alpha L)^2} (\varphi^{(P)} - 1) \tag{13}$$

On the other hand tip rotation is given as

$$\theta_{II}^{(P)} = \left(\frac{PL^2}{EI} \right) \times \left[\left(\frac{\cos \alpha L - 1}{(\alpha L)^2} \right) + \varphi^{(P)} \times \left(\gamma \cos \alpha L + \frac{\sin \alpha L}{(\alpha L)} \right) \right] \tag{14}$$

Shortly the ratio of these two expressions yield the following formula

$$\frac{\theta_{II}^{(P)}}{\theta_{II,chord}^{(P)}} = \left(\frac{\cos \alpha L - 1}{\varphi^{(P)} - 1} \right) + \varphi^{(P)} (\alpha L) \left(\frac{\gamma (\alpha L) \cos \alpha L + \sin \alpha L}{\varphi^{(P)} - 1} \right) \tag{15}$$

The graphical representation of this ratio is presented in Fig. C.c

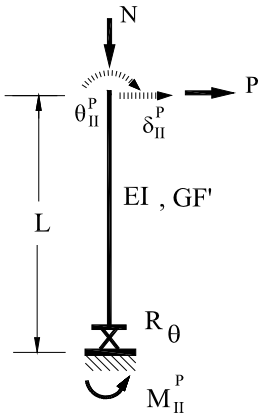

a. Column subjected to P and N : second order analysis

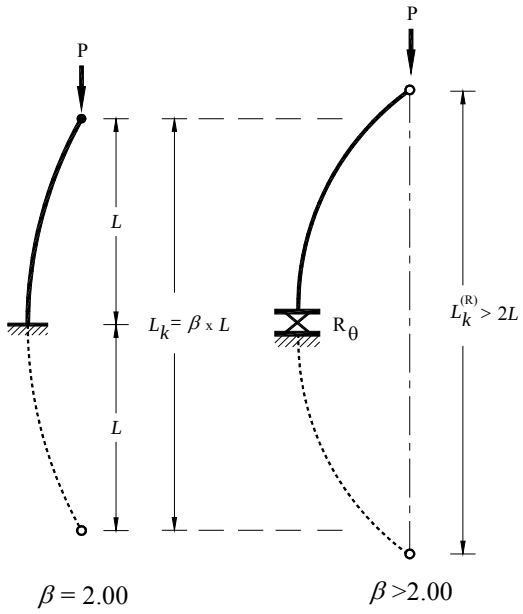

b. Graphical representation

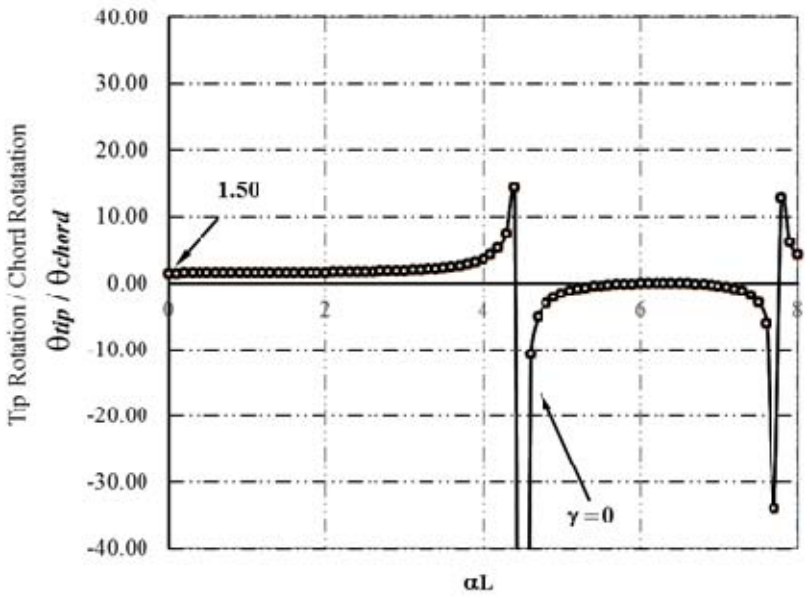

c. Ratio of Tip Rotation to Chord Rotation for fully restrained Cantilever Column (γ=0)

Fig C